# COMPACT XFEL LIGHT SOURCE*

W.S. Graves#, K.K. Berggren, S. Carbajo, R. Hobbs, K.-H. Hong, W.R. Huang, F.X. Kärtner, P.D. Keathley, D.E. Moncton, E. Nanni, K. Ravi, M. Swanwick, L.F. Velásquez-García, L.J. Wong, Y. Yang, L. Zapata, Y. Zhou, MIT, Cambridge, MA, USA
J. Bessuille, P. Brown, E. Ihloff, MIT-Bates Laboratory, Middleton, MA, USA
S. Carbajo, J. Derksen, A. Fallahi, F.X. Kärtner, F.Scheiba, X.Wu, CFEL-DESY, Hamburg, Germany
D. Mihalcea, Ph. Piot, I. Viti, N. Illinois University, Dekalb, IL, USA

*Abstract*

X-ray free electron laser studies are presented that rely on a nanostructured electron beam interacting with a "laser undulator" configured in the head-on inverse Compton scattering geometry. The structure in the electron beam is created by a nanoengineered cathode that produces a transversely modulated electron beam. Electron optics demagnify the modulation period and then an emittance exchange line translates the modulation to the longitudinal direction resulting in coherent bunching at x-ray wavelength.

The predicted output radiation at 1 keV from a 7 MeV electron beam reaches 10 nJ or $6X10^8$ photons per shot and is fully coherent in all dimensions, a result of the dominant mode growth transversely and the longitudinal coherence imposed by the electron beam nanostructure. This output is several orders of magnitude higher than incoherent inverse Compton scattering and occupies a much smaller phase space volume, reaching peak brilliance of $10^{27}$ and average brilliance of $10^{17}$ photons/(mm$^2$ mrad$^2$ 0.1% sec). The device is much smaller and less expensive than traditional XFELs, requiring electron beam energy ranging from 2 MeV to a few hundred MeV for output wavelengths from the EUV to hard x-rays. Both laser and THz radiation may provide the undulator fields.

## INTRODUCTION

In the course of investigating coherent inverse Compton scattering (ICS) from a nanostructured electron beam [1] it has been found that under certain conditions FEL gain occurs, and that this interaction has significant positive effects on the properties of the radiation emitted. FEL gain for a laser undulator has been previously predicted and studied [2,3] but for very different sets of electron beam and laser parameters than are presented here. In this case the bunch charge and peak current are much lower than earlier studies, as is the electron beam emittance. Furthermore by creating a pre-bunched electron beam via a structured cathode and emittance exchange, the number of gain lengths required to saturate is much reduced, which in turn eases the power, focusing and pulse length requirements on the laser.

*Supported by DARPA N66001-11-1-4192, CFEL DESY, DOE DE-FG02-10ER46745, DOE DE-FG02-08ER41532, and NSF DMR-1042342.
#wsgraves@mit.edu

The net effect of these changes is to allow an XFEL based on collision of a low energy electron beam with a laser that is within present state-of-the-art technologies and results in a very compact and inexpensive x-ray laser. A facility to test these ideas is currently under construction within the DARPA Axis program and is described below. First though the conditions for FEL gain are reviewed as is the method of producing the nanostructured electron beam.

## FEL GAIN

For head-on ICS the resonance condition is given by

$$\lambda_x = \frac{\lambda_L}{4\gamma^2}\left(1+\frac{a_0^2}{2}\right) \quad (1)$$

where $\lambda_x$ is the x-ray wavelength, $\lambda_L$ is the laser wavelength, $\gamma$ is the relativistic factor, and $a_0 \quad \frac{eE_L\lambda_L}{2\pi mc^2}$ where $E_L$ is the laser electric field. The Pierce parameter that determines many of the FEL properties is given by

$$\rho_{fel} \quad \frac{1}{2\gamma}\left(\frac{I}{I_A}\frac{\lambda_L^2 a_0^2}{8\pi^2\sigma_x^2}\right)^{1/3} \quad (2)$$

where $\sigma_x$ is the electron beam size, $I$ is the peak current, and $I_A$ = 17,045 A is the Alfen current. A Bessel function factor in Eq. 2 has been dropped because its value is very close to unity for $a_0^2 \ll 1$ which is true for the present case. The 1D e-folding length for FEL gain is

$$L_G \quad \frac{\lambda_L}{8\pi\sqrt{3}\rho_{fel}} \quad (3)$$

The design goal for the FEL is to have $\rho_{fel}$ large and $L_G$ small. One of the advantages of using a laser undulator is seen in the very short gain lengths possible due to the short period relative to a static undulator.

It is useful to solve Eq. 1 for $\lambda_L$ with the assumption $a_0^2 \ll 1$ and substitute into Eq. 2 to find how the Pierce parameter scales with electron energy $\gamma$, peak current $I$, and x-ray wavelength $\lambda_x$. The beam size is also replaced with $\sigma_x^2 \quad \frac{\varepsilon_{xN}\beta_x}{\gamma}$ , yielding

$$\rho_{fel} \quad \left(\frac{I}{I_A}\frac{\gamma^2\lambda_x^2 a_0^2}{4\pi^2\varepsilon_{xN}\beta_x}\right)^{1/3} \quad (4)$$

ISBN 978-3-95450-126-7

Thus for the compact XFEL a low emittance electron beam and a small focus at the interaction point must be used to offset the small $\gamma$ that results from a short undulator period and the low peak current consistent with that energy. Both of these goals, low emittance and a tight focus, are achievable by scaling to low charge per bunch and using short laser pulses at a tight focus.

In order for the gain length to obey Eq. 3 several conditions due to 3D effects of the electron and x-ray beams must be met. The electron beam energy spread must satisfy

$$\left(\frac{\Delta\gamma}{\gamma}\right)_{rms} \equiv \delta < \rho_{fel} \tag{5}$$

in order to allow coherent bunching. The normalized emittance must satisfy

$$\varepsilon_{xN} \le \frac{\gamma\lambda_x}{4\pi}\left(\frac{\beta_x}{L_G}\right) \tag{6}$$

The term in brackets is often ignored in high energy XFELs using a conventional undulator where the gain length is tens of centimeters.. In that case best gain is achieved for $\beta_x \approx L_G$, but as will be shown below the gain length for the current case is tens of microns while the beta function is hundreds of microns so that the emittance requirement for an XFEL with laser undulator is significantly eased relative to a conventional XFEL. This effect is due to gain guiding where the fundamental mode experiences fast growth before diffracting away while the higher order modes diffract at larger angles. To avoid reduction of gain due to diffraction outside the electron beam, the gain length must be less than the x-ray Rayleigh length

$$L_G \le Z_R^{xray} = \frac{4\pi\sigma_x^2}{\lambda_x} \tag{7}$$

which is easily met in practice for the very short gain lengths under study.

The scaling above apply to SASE and seeded FELs. Here a third type of FEL is presented that uses an electron beam with a coherently modulated ("prebunched") current generated prior to the FEL interaction. Upon entering the laser field this electron beam emits superradiantly at the resonance wavelength and then undergoes FEL gain as for the other cases. The next section describes the generation of the modulated electron beam.

## MODULATED ELECTRON BEAM

The modulated electron beam is created by emission of discrete beamlets from a nanostructured cathode, acceleration to relativistic energy, and then emittance exchange of the beamlet structure from the transverse phase space plane into the longitudinal plane. Figure 1 shows several types of nanostructures that have been fabricated and tested at MIT. These early explorations are investigating different geometries, fabrication techniques, and materials to find the best beam characteristics at high

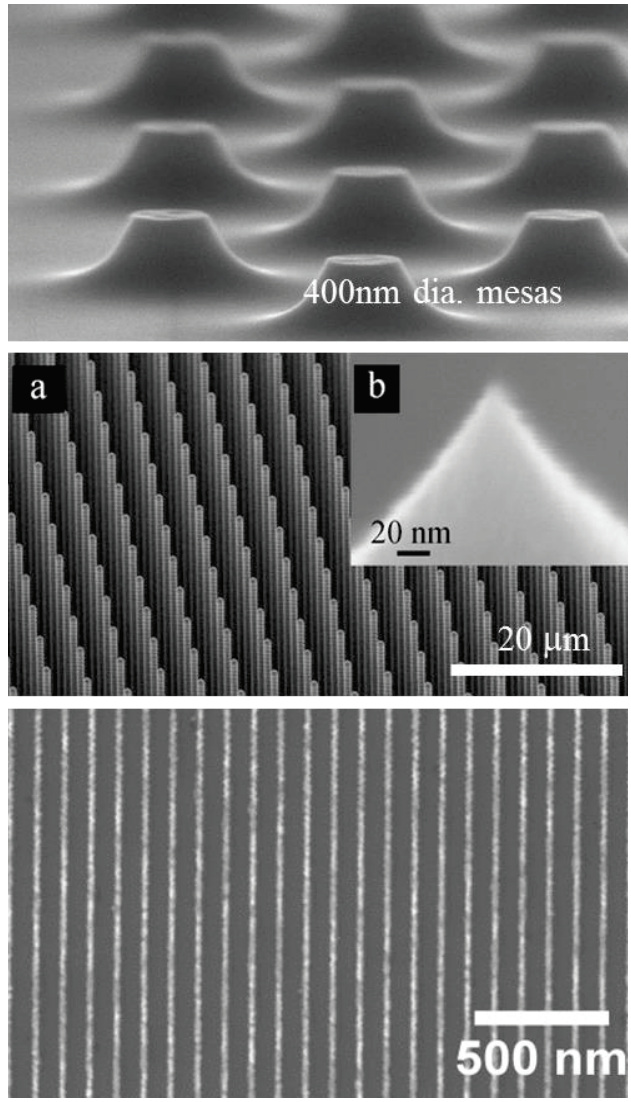


Figure 1: Top shows Si mesas with wide emitting areas suitable for photoemission. Middle shows high aspect ratio Si pillars with 4.4 nm tips [4]. Bottom shows Au lines each 18 nm at 100 nm pitch.

energy, and so a variety of cathodes are under consideration. The upper plot of Fig 1 shows low aspect ratio mesas fabricated of n-doped Si. The diameter and pitch of the mesas may be varied over a wide range, from hundreds of microns down to tens of nanometers. The flat mesa surface is suitable for photoemission from a well-defined emitter size. The middle plot shows high aspect ratio doped Si pillars with a pitch of 5 μm and tip diameter 4.4 ± 0.6 nm [4]. These tips have been tested in DC fields over a range of IR laser energies resulting in multiphoton emission, and scaling up to optical field emission at higher laser intensity. The array of tips has produced charge densities up to 45 pC/mm$^2$ per shot from an array of ~2,220 tips at modest DC field. The 2,220 tip array has generated 1.2 pC/shot at 3 kHz for 8 million continuous cycles. No damage is evident in subsequent SEM micrographs [5].



ISBN 978-3-95450-126-7

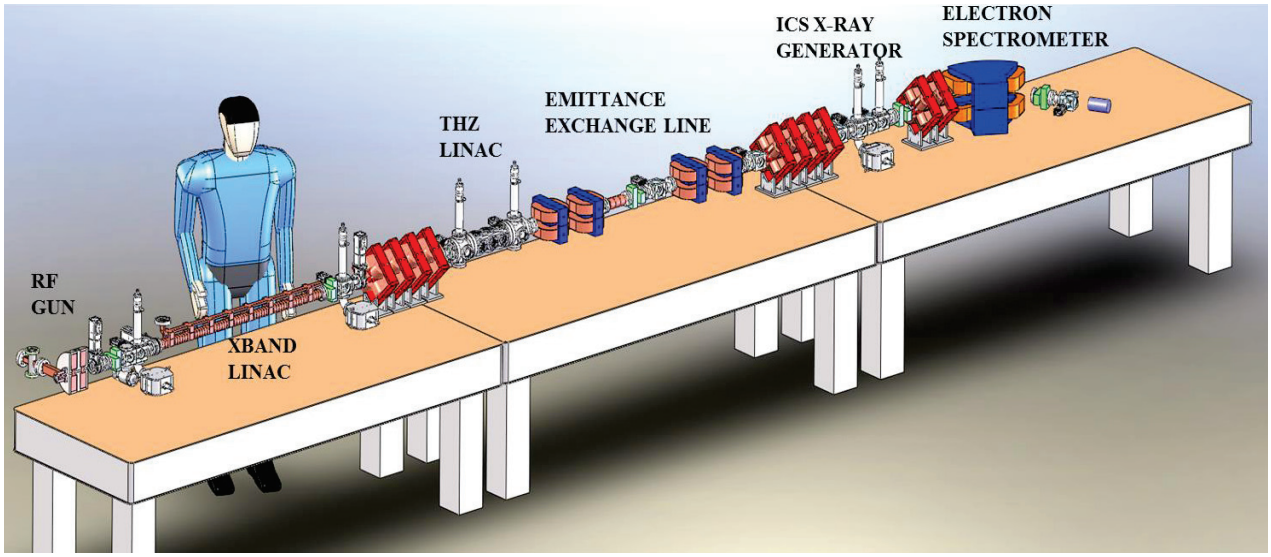


Figure 2: Layout of prototype currently under construction. Major components are labeled and shown mounted on optical tables. Structure is less than 5 m long and will be commissioned in early 2014.

The lower image in Figure 1 shows fabricated Au lines instead of tips. The lines are interesting because the effective packing factor is increased and the emittance exchange technique only depends on structure in one dimension. These lines have been fabricated via electron beam lithography which is capable of creating lines down to 10 nm width with pitch of <50 nm. Because the pitch at the cathode is eventually transformed into longitudinal period at x-ray wavelength it is desirable to start with a small pitch. The emittance exchange technique is essentially demagnifying and reimaging the cathode in a different dimension. Note that a large demagnification is possible due to acceleration to relativistic energy. Aberrations in the imaging process eventually limit the minimum x-ray wavelength achievable but there is a favourable scaling at relativistic energy. The image fidelity is set by the range of trajectories that the magnet optics can collect and focus. The large angular spread at the cathode is decreased by the ratio of $\beta\gamma_{cathode}/\beta\gamma_{final} \approx 10^{-4}$ after acceleration so that large demagnification is possible. Note that the modulation pitch after the EEX may be varied simply by varying the transverse beam size before EEX via quadrupole focusing.

A variety of laser triggered emission mechanisms are being investigated including linear photoemission, multi-photon emission, and optically assisted field emission. For the purposes of determining emittance it will be assumed that scaling of planar photoemission [6] can be used. The nonplanar surface of small tips may lead to a larger collection of angles emitted but this will exhibit a correlation of angle with position on the tip, which does not necessarily produce a larger emittance. Furthermore due to the very small dimensions of the tips, the nanocathode array may actually have lower surface roughness than a conventionally polished planar cathode. An experimental chamber to measure the tip emittance is now under construction. The emittance of a single tip will be exchanged into the longitudinal plane and constitute a single nanobunch at the x-ray wavelength. To relate the properties of an upright nanobunch ellipse downstream of the EEX to the upstream transverse nanotip emittance we write

$$\varepsilon_{Ntip} = \gamma\sigma_z\delta \tag{8}$$

where the nanobunch length should be a fraction of the x-ray wavelength. The energy spread $\delta$ must satisfy Eq. 5.

## PROTOTYPE FACILITY

A facility to test coherent x-ray output from modulated electron beams in now under construction and is shown in Figure 2. It consists of 3 RF structures – gun, linac, and RF deflector – all operating at 9.3 GHz and 1 kHz repetition rate. The RF structures were developed in collaboration with SLAC. The 2.5 cell x-band gun is optimized for high efficiency, high cathode field and low field in the coupler cell. Superfish and HFSS models indicate 150 MV/m gradient for 2 MW RF power and a resulting beam energy of 2.1 MeV. The fill time is 100 ns allowing short RF pulses to be used, and enabling high repetition rate. Two solenoids are just downstream of the gun with equal strength but opposite polarity in order to symmetrically focus the beam without causing rotation about the z-axis. A short 1 m long linac operates with a gradient of 20 MV/m and 20 MeV energy gain for 3 MW input power. A chamber for testing of THz acceleration follows the x-band linac and will be used to boost the electrons to higher energy. A group of 2 quadrupole doublets then matches the transverse phase space into the EEX line to provide upright longitudinal ellipses downstream. The EEX line consists of 2 doglegs, each with dispersion of 7.2 cm separated by a 9 cell RF deflector that generates 1.45 MV transverse voltage for 0.5 MW input power. Following the EEX line another

ISBN 978-3-95450-126-7

group of 2 quadrupole doublets focuses the electron beam at the interaction point (IP). The doublets are designed to provide a $\beta^*$ at the IP as low as 0.2 mm. The entire accelerator and transport line is less than 5 m long and consists of a small number of components. The very stable optical, thermal, mechanical, and electrical requirements can be met at modest cost due to the small size. The electron energy is so low that synchrotron radiation effects on the beam are negligible. Although care is needed in handling and transport of the low energy beam, the short accelerator simplifies the physics and has significant advantages over a large machine.

The primary laser is a cryo-cooled Yb:YLF amplifier producing 100 mJ pulses of 1 μm light at 100 Hz, upgradeable to 1 kHz. The bandwidth limited pulse length is 500 fs. Because the FEL gain bandwidth is narrow, of order $10^{-3}$, it is important to keep the laser intensity constant within that factor over the interaction length. Various schemes have been proposed [3, 7] to ensure a constant intensity. These and other methods will be explored to keep a constant resonant condition with intensity parameter $a_0 = 0.4$.

## XFEL PERFORMANCE

The compact XFEL is tunable over a wide wavelength range per Eq. 1 by varying the electron beam energy. At 2 MeV from the gun, the output photon energy is 90 eV (13 nm) , and scales up to 8 keV (0.15 nm) at the linac exit energy of 22.5 MeV. An example FEL interaction is worked at 1 keV photon energy in order to illustrate the design beam parameters and performance. From Eq. 1 with a 1μm laser, a0 = 0.4, and 1.24 nm output wavelength, the resulting $\gamma = 15$ and the electron energy is 7 MeV. The 1.3 ps laser contains 400 periods. The beta function at the IP is set to 300 μm, close to the interaction length. In order to find the emittance that satisfies Eq. 6 we must calculate the gain length $L_G$ using Eqs. 3 and 4, which yield $L_G$ = 32 μm. The very short gain length is due to the short undulator period and shows one of the advantages of using laser undulators. With such a short gain length the factor in brackets in Eq. 6 significantly relaxes the emittance requirement relative to a GeV energy conventional FEL. The required emittance is then $\varepsilon_{xN} < 15$ nm. The standard photocathode emittance scaling is 250 nm per mm edge (not RMS) radius so that a laser spot no larger than 40 μm radius will produce the required emittance of ~10 nm. Allowing for some emittance growth during acceleration and transport, a cathode radius of 30 μm is chosen. The charge per bunch is limited by space charge according to $Q \le \pi r^2 \varepsilon_0 E_{RF} \sin(70^\circ)$ where $E_{RF}$ is the cathode gradient and 70° is the start phase, so that $Q \le 3.5$ pC. Parmela simuations indicate that the emittance of the global beam and nanobunch are preserved through the gun exit, the most critical phase for emittance growth due to space charge. With an initial energy of 0.5 +/- 0.3 eV the global thermal emittance is 9.0 nm and the nanotip emittance is 5.7 pm. At the gun exit energy of 2.16 MeV, the global emittance is 10.6 nm and the nanobunch emittance is 6.7 pm.

With these values and a peak current of 70 A after EEX the Pierce parameter $\rho_{fel} = 7\text{X}10^{-4}$ and the FEL gain length is 32 μm. It is perhaps surprising that the Pierce parameter for this modest peak current and low energy is similar to multi kA XFELs operating at GeV energy. From Eq. 4 it is seen that the small emittance and beta function in the denominator offset the small current and energy in the numerator. This set of choices for beam parameters is far more attainable than the much higher current, charge, and moderate emittance proposed by other groups.

The saturation power is $P_{sat} \quad \rho I \gamma mc^2 = 350$ kW. For 70 A current with 2 pC charge, the pulse length is 30 fs. Note that with the chosen geometry, the R62 matrix element of the EEX line provides about an order of magnitude bunch compression (from x to z) so that this short pulse length is straightforward to attain. Multiplying power by pulse length, the total x-ray pulse energy is 10 nJ or $6\text{X}10^8$ photons. There are $10^7$ electrons in the bunch so that each electron emits about 60 photons or ~4 orders of magnitude higher flux than incoherent Compton scattering. This performance yields peak brilliance of $10^{27}$ and average brilliance of $10^{17}$ photons/(mm$^2$ mrad$^2$ 0.1% sec). Note that if the same process were used with a compact superconducting linac the average brilliance would increase to ~$10^{22}$, similar to 3rd generation synchrotrons, while the peak brilliance would fall by an order of magnitude due to lower laser power per pulse. The electron beam and estimated x-ray properties are shown in Tables 1 and 2.

Table 1: Electron Beam Parameters

| | |
|---|---|
| Charge [pC] | 2 |
| Bunch length [fs] | 28 |
| Peak current [A] | 70 |
| Energy spread [%] | 0.01 |
| Spot size at IP [μm] | 0.5 |
| Emittance [nm] | 10 |
| Repetition rate [Hz] | 1000 |
| Energy [MeV] | 7 |

Table 2: X_ray Parameters

| | |
|---|---|
| Photon energy [keV] | 1 |
| Pulse energy [nJ] | 10 |
| Photons/pulse | $6\text{X}10^8$ |
| Photons/sec | $6\text{X}10^{11}$ |
| Source size [μm] | 0.5 |
| Source divergence [μrad] | 200 |
| Peak brilliance [phot/s 0.1% mm$^2$ mrad$^2$] | $10^{27}$ |
| Avg brilliance [phot/s 0.1% mm$^2$ mrad$^2$] | $10^{17}$ |



ISBN 978-3-95450-126-7

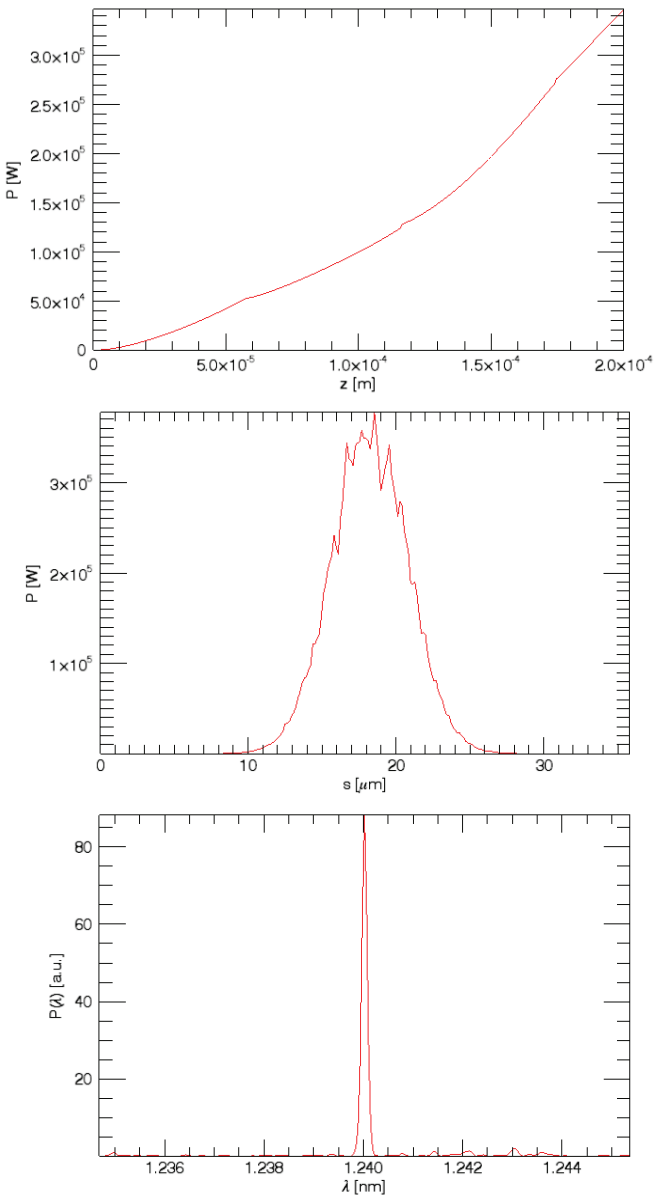


Figure 3: Results from GENESIS simulations. Top shows power growth to 350 kW over an interaction length of 200 microns. Middle shows time profile of short x-ray pulse. Bottom shows near transform-limited spectrum with a linewidth of 0.02%.

Initial results for time dependent simulations with the 3D FEL code GENESIS are shown in Figure 3. The simulations use the electron and laser parameters derived in the previous sections and summarized in Table 1. A 1.3 ps long laser pulse is used, resulting in a 200 μm interaction length (half the laser pulse length since the beams are counter propagating), which is ~6 gain lengths. The power curve is still rising and has not yet saturated as seen in the top plot of Figure 3. The middle plot of Figure 3 shows the output x-ray time profile with a pulse width similar to the electron bunch length. The power peaks at 350 kW although from the growth curve it doesn't appear to have fully saturated yet. The spectrum consists of a single spike with width close to the transform limit. This is due to the coherent modulation provided by the nanostructured cathode and emittance exchange, which effectively seed the x-ray output.

## CONCLUSIONS

It has been shown that FEL gain is possible in an inverse Compton scattering experiment for a set of electron and laser beam parameters that are achievable with current technology. Combining FEL gain with a modulated electron beam from a nanocathode opens the possibility for fully coherent x-rays from a compact device. The conditions for lasing have been derived and an example worked for 1 keV photons that predicts 10 nJ/pulse output. Although the physics is clear, challenges remain, primarily in achieving the necessary stability in the laser and accelerator operations. A compact facility is under construction at MIT to test the ideas presented. Such a device can bring ultrafast x-ray science into a wide range of university and industry laboratories. In addition it may prove useful as a stable and fully coherent seed source for large XFELs.

## REFERENCES

[1] W.S. Graves, P. Piot, F.X. Kärtner, D.E. Moncton, "Intense Superradiant X Rays from a Compact Source Using a Nanocathode Array and Emittance Exchange," Phys Rev Lett 108, 263904 (2012).

[2] A.Bacci, M. Ferrario, C. Maroli, V. Petrillo, L. Serafini, "Transverse effects in the production of x rays with a free-electron laser based on an optical undulator", Phys. Rev. ST Accel. Beams 9 060704 (2006).

[3] P. Sprangle, B. Hafizi, J.R. Penano, "Laser-pumped coherent x-ray free-electron laser", Phys. Rev. ST Accel. Beams 12 050702 (2009).

[4] M. Swanwick, P.D. Keathley, F.X. Kärtner, L.F. Velásquez-García, "Ultrafast Photo-Triggered Field Emission Cathodes Using Massive, Uniform Arrays of Nano-Sharp High-Aspect-Ratio Silicon Structures",Tech. Digest of the 17th Intl Conf on Solid-State Sensors, Actuators, and Microsystems, Barcelona, Spain, pp. 2680 – 2683, June 16 – 20 2013.

[5] M. Swanwick, P.D. Keathley, F.X. Kärtner, and L.F. Velasquez-Garcia, "Nanostructured Silicon Photocathodes for X-ray Generation", Tech. Digest of the 26th International Vacuum Nanoelectronics Conf, Roanoke VA, July 2013.

[6] D.H. Dowell and J.F. Schmerge, "Quantum efficiency and thermal emittance of metal photocathodes", Phys. Rev. ST Accel. Beams 12, 074201 (2009).

[7] C. Chang, C. Tang, J. Wu, "High-GainThomson-Scattering X-Ray Free-Electron Laser by Time-Synchronic Laterally Tilted Optical Wave", Phys. Rev. Lett. 110, 064802 (2013).

ISBN 978-3-95450-126-7